

## Elastic recoil detection analysis with heavy ions

W. Assmann \*, H. Huber, Ch. Steinhausen, M. Dobler, H. Glückler, A. Weidinger <sup>1</sup>

*Sektion Physik, Universität München, 85748 Garching, Germany*

Detection of elastically scattered recoils instead of projectiles offers the possibility to unambiguously identify sample components and is still a quantitative method for materials analysis. Large electrostatic accelerators delivering high energetic heavy ion beams of excellent quality and large area ionization detectors with particle and position resolution are shown to be a very suited combination to fully utilize the potential of the ERDA method. Using 170 MeV I or 200 MeV Au beams a sensitivity below  $10^{14}$  atoms/cm<sup>2</sup> and depth resolution below 10 nm were obtained with 7.5 msr detector solid angle. The position resolution enables the correction of kinematic energy shifts and, in addition, the observation of blocking patterns from single crystalline materials.

### 1. Introduction

Ion beam analysis was shown to be a valuable tool for surface and thin film analysis. First of all Rutherford backscattering spectrometry (RBS) with light ions, typically 1–3 MeV p or He ions, is a successful and often used technique for depth profiling of element concentration [1]. Furthermore under channeling conditions it gives information on the structure of thin layers [2]. RBS is a simple and fast method, which has one essential advantage compared to most analyzing techniques, it is quantitative. The areal density of a certain element, i.e. the number of atoms per cm<sup>2</sup>, can be deduced from the measurement of elastically scattered ions using Rutherford formula without any further calibration. Of course the RBS technique has also its limitations. Mass resolution for heavy elements and sensitivity for light elements are poor, and except for the surface, mass determination is not unambiguously possible. Weak concentrations of elements cannot be detected, if their energy distribution is overlapped by other strong components in the sample. The mass resolution of RBS can be improved with beams of higher energies or heavier ions, but to overcome the other limitations mentioned, different ion beam techniques have to be used, e.g. PIXE (proton induced X-ray emission) or NRA (nuclear reaction analysis) [3]. But there exists a physical complement to RBS, which allows unambiguous particle identification saving the quantitative feature: elastic recoil detection analysis (ERDA).

Originally it was developed for H detection [9] or light element profiling [5,6] with an absorber foil in

front of the energy detector for beam suppression. Subsequent advanced versions of ERDA used various detection methods with particle identification capabilities to avoid this absorber foil and the connected difficulties. Time-of-flight (TOF) systems [7,8], magnetic spectrometers [9,10] and different kinds of particle telescopes have been applied for this purpose [11–15]. In most cases medium heavy ion beams, typically <sup>36</sup>Cl ions, have been used for ERDA so far with energies around 30 MeV. But Stoquert et al. [16] have demonstrated the large potential of this method, if a 16 MV tandem accelerator and corresponding high energetic heavy ion beams are available. Their work partly influenced our intention at the Munich accelerator laboratory to use our 14 MV tandem accelerator for materials analysis. It is the aim of this paper to point out the special possibilities of large electrostatic accelerators in surface and thin film analysis with the ERDA technique.

First we will summarize the principles of ERDA and give specific arguments of using very heavy ions for this method. The depth resolution dependence on the detection geometry will be discussed in more detail. Then the experimental setup we use at the Munich accelerator laboratory will be described including a large area ionization detector system with particle and position resolution. With typical examples of ERDA we will illustrate in the last part, which results can be achieved by simple energy detection of recoils as well as by sophisticated detection methods with particle and position resolution.

### 2. Basic principles of ERDA

The physical basis which has given the method its name is elastic scattering of incident ions on a sample

\* Corresponding author.

<sup>1</sup> Permanent address: Hahn-Meitner-Institut 14109 Berlin, Germany.

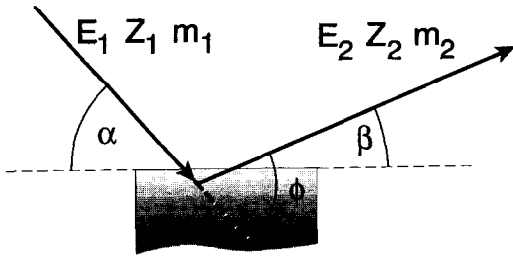


Fig. 1. Schematic diagram of the ERDA geometry.

surface and detecting the recoiling sample atoms, typically in reflexion geometry, as shown in Fig. 1. The scattering process can be described by simple expressions, if the projectile energy is within the range, where Rutherford scattering can be assumed. A detailed discussion of the measured energy spectra dependency on beam parameters and geometry can be found in ref. [16], here we will give only a short summary with special emphasis on the heavy ion aspect. The energy  $E_2$  transferred by projectile ions of mass  $m_1$  and energy  $E_1$  to sample atoms of mass  $m_2$  recoiling at an angle  $\phi$  with respect to the incidence direction is given by:

$$E_2 = \frac{4m_1m_2}{(m_1 + m_2)^2} E_1 \cos^2\phi. \quad (1)$$

Eq. (1) can also be written as:

$$\frac{E_2}{m_2} = \frac{4 \cos^2\phi}{(1 + m_2/m_1)^2} \frac{E_1}{m_1}, \quad (2)$$

i.e. for ERDA with very heavy ions, where  $m_2/m_1 \ll 1$ , all recoiling ions have similar velocities. Therefore the stopping power, which depends on the particle velocity, is in the same regime for all recoils. We will come back to this point later in the discussion of particle resolution with ionization detectors. From the corresponding formula of the energy angle correlation of the scattered projectiles a maximum scattering angle  $\theta'_{\max}$  can be deduced for  $m_1 > m_2$ :

$$\theta'_{\max} = \arcsin(m_2/m_1). \quad (3)$$

Thus with heavy ion beams in most cases scattered projectiles can be prevented from reaching the detector, making absorber foils unnecessary.

The differential elastic recoil cross section  $\sigma_{\text{ERD}}$  is given by:

$$\sigma_{\text{ERD}} = \left( \frac{Z_1 Z_2 e^2}{2E_1} \right)^2 \left( \frac{m_1 + m_2}{m_2} \right)^2 \cos^{-3}\phi, \quad (4)$$

where  $Z_1$  and  $Z_2$  are the atomic numbers of projectile and sample atoms, respectively. For  $m_2/m_1 \ll 1$  and with the approximation  $m = 2Z$  in Eq. (4) two essential consequences can be seen, first the sensitivity is

roughly the same for all elements and secondly it has a  $Z_1^4$  dependence on the projectile ion [17]. Thus very low beam currents can be used in heavy ion ERDA, avoiding excessive sample heating.

Special attention has to be given to beam induced damage (sputtering or amorphization) with heavy ions. If only nuclear interaction is taken into account, it has been shown [18,10] that the ratio of recoiling to displaced atoms is independent of  $Z_1$  and only weakly dependent on the projectile mass. But there are enhanced sputter yields with high energetic heavy ions known for nonmetallic materials [19] as well as enhanced radiation damage in high  $T_c$  superconductors [20] probably due to electronic effects. Therefore very heavy ion beams might be disadvantageous for certain materials and lighter ions should be used. In any case the acceptance angle of the detector system should be as large as possible to minimize the radiation damage.

This demand however is in conflict with the requirement of optimum depth resolution usually, which follows from the depth resolution dependency on the detection geometry. In the surface approximation and assuming constant energy loss the depth resolution  $\delta x$  can be written:

$$\delta x = \frac{\delta E_2}{E_2} (S_{\text{rel}})^{-1}, \quad (5)$$

where  $S_{\text{rel}}$  is the relative energy loss factor defined by:

$$S_{\text{rel}} = \frac{dE_1/dx}{E_1} \frac{1}{\sin \alpha} + \frac{dE_2/dx}{E_2} \frac{1}{\sin \beta}. \quad (6)$$

$\alpha$  and  $\beta$  are the incidence angle of the beam and exit angle of the recoiling ion, respectively, connected to the scattering angle  $\phi$  by  $\phi = \alpha + \beta$ . It should be noticed here that the depth resolution depends on the relative energy resolution only, as well as the relative stopping power of incoming and outgoing ions. Essential contributions to the energy spread  $\delta E$ , which can be influenced, are the detector resolution and the energy broadening due to the measuring geometry. The detector acceptance angle and the finite beam spot size define a scattering angle range  $\delta\phi$  causing a kinematic energy spread  $\delta E_{\text{kin}}$  according to:

$$\delta E_{\text{kin}} = 2E_2 \tan \phi \delta\phi. \quad (7)$$

A detailed analysis of the different contributions to depth resolution shows [16] that this kinematic effect is the predominant term near the surface, severely limiting the permitted detector acceptance angle, whereas energy straggling dominates the resolution at larger depth. If we estimate  $\delta\phi$  for a scattering angle of  $37.5^\circ$  causing a kinematic energy shift comparable to typical detector energy resolutions of 1%, the angular spread  $\delta\phi$  has to be less than  $0.4^\circ$ . The beam spot size contribution to the angular spread can easily be kept in this range, but the detector solid angle involved is

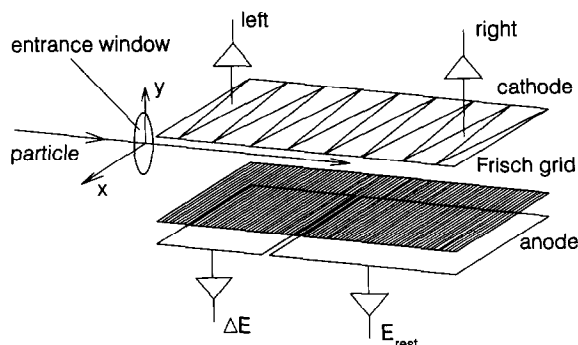


Fig. 2. Schematic view of ionization detector layout.

0.04 msr only. Therefore a detector system with large solid angle as well as high depth resolution must enable corrections for the kinematic energy shift.

### 3. Detector and setup for HIERDA

Large area ionization chambers with particle and position resolution have been used since many years for nuclear physics experiments and can be easily adapted to any specific geometry. Detectors of such a kind seemed to us the best suited for our new ERDA installation at the Munich accelerator laboratory [21,22]. The often used TOF spectrometers with solid state detectors for energy detection are restricted to small solid angles. A detailed description of our ERDA detector is given in ref. [23], briefly, it is a transversal field ionization chamber of 28 cm active length with Frisch grid and subdivided anode electrode (Fig. 2). From the anode signals  $\Delta E$  and  $E_{\text{rest}}$  the total energy  $E_{\text{tot}} = \Delta E + E_{\text{rest}}$  as well as the atomic number  $Z$  can be deduced. The detector gas used is isobutane at pressures of 20–90 mbar with electronically regulated constant flow. The entrance window consists of a grid supported stretched polypropylene foil with  $50 \mu\text{g}/\text{cm}^2$  typical thickness. It has to be noted that the foil thickness homogeneity is of more importance for the detector energy resolution than the absolute thickness. The energy loss variation due to different foil thicknesses can easily surpass the effect of energy loss straggling especially if heavy ions are detected. The cathode electrode is divided in two insulated halves with “backgammon” shape (see Fig. 2), thus charges induced at the right and left half give information on the entrance position of the particles. The  $x$  coordinate can be derived from the corresponding charges  $l$  and  $r$  according to  $x = (l - r)/(l + r)$ , whereas the  $y$  coordinate results from  $y = (l + r)/E_{\text{tot}}$  because of the position independence of the anode pulses. For transformation of the  $(x, y)$  information into scattering angle  $\phi$  a removable calibration mask in front of the en-

trance window is used which allows to correct for  $x$  and  $y$  distortions too. An example of such a calibration measurement is shown in Fig. 3 corrected only in the scattering plane ( $x$  position). It should be mentioned that the ion drift time to the cathode is of the order of some ms, therefore to avoid pulse pileup the number of particles entering the detector has to be limited to 1 kHz. The ionization detector can be connected to the scattering chamber at different ports, corresponding to scattering angles of 12.5, 25, 37.5 and 50 degr. (see Fig. 4).

The essential part contained in the 45 cm diameter vacuum chamber is a sample positioning system with computer controlled stepper motors which allows linear sample movements in all three dimensions and rotation around an axis perpendicular to the scattering plane. This system is necessary for changing the incidence angle of the beam on the sample surface without moving the beam spot. Sample transfer is done by use of a load lock system without breaking the chamber vacuum. In spite of the positioning system originally not designed for vacuum conditions, basic pressures of  $1 \times 10^{-7}$  mbar could be reached in the scattering chamber.

Another smaller vacuum chamber is installed in front of the ERDA chamber, mainly for RBS measurements. This chamber contains besides a rotatable target wheel for RBS samples a second wheel, which can be used for ERDA of thin foils in transmission geometry (Fig. 4). In this version of ERDA, only the energy of the recoils is measured. Because of the limited lifetime of solid state detectors with heavy ions we use cheap PIN diodes for this purpose, which have sufficient energy resolution [24]. This second target wheel gives us also a possibility for beam current determina-

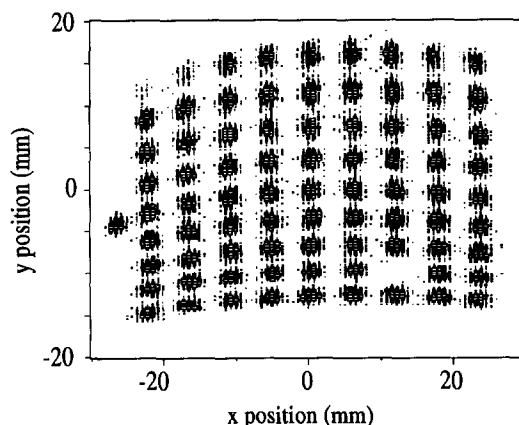


Fig. 3. Two-parameter plot of  $(x, y)$ -position measurement with calibration mask at the entrance window. The mask has a pattern of 2 mm diameter holes with 6 mm  $x$ -spacing and 4 mm  $y$ -spacing. The  $y$  distortion is a measuring effect (see text).

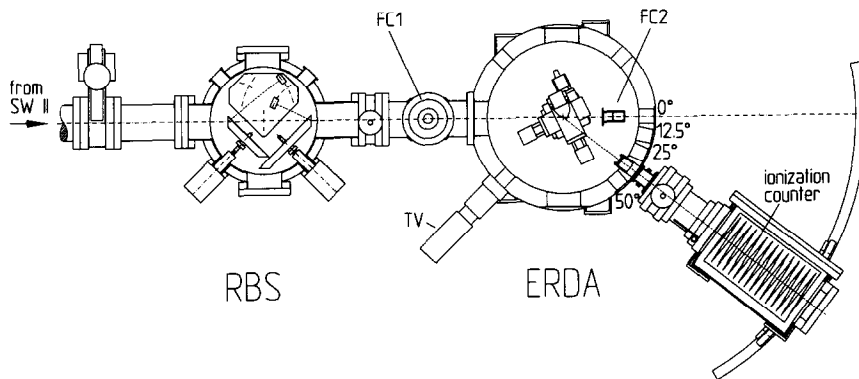


Fig. 4. Schematic diagram of the RBS/ERDA setup. The use of the RBS chamber for ERDA in transmission geometry is indicated. The beam is adjusted by use of Faraday cups FC1/2 and a TV camera.

tion, if absolute concentrations should be measured. In this case a monitor foil ( $2 \mu\text{g}/\text{cm}^2$  Au on  $10 \mu\text{g}/\text{cm}^2$  C) is mounted on this wheel and the scattered particles are detected with a PIN diode. The monitor count rate is calibrated using a Faraday cup with secondary electron suppression.

#### 4. ERDA with $E$ detection

ERDA in transmission geometry, where only the energy of the recoiling sample atoms is measured, was extensively used for contamination analysis of target foils for nuclear physics experiments. Target contaminations can be a severe problem especially if strong contaminant reactions are interfering with weak reaction channels to be studied. An example are self-supporting  $^{100}\text{Mo}$  targets, which have been fabricated using a newly developed high vacuum sputter deposition process [25]. Foils of typically  $100 \mu\text{g}/\text{cm}^2$  thickness have been analyzed with  $140 \text{ MeV } ^{127}\text{I}$  ions at  $37^\circ$  scattering angle detecting the energy of scattered particles in a  $220 \mu\text{m}$  thick PIN diode. The energy spectrum (Fig. 5) showed besides peaks corresponding to Mo recoils and I projectiles scattered on Mo a surprisingly high C contamination of 20 to 100 at.% in different foils. In the experiments where these targets should be used nuclear reactions on C would create an intolerable high background. The C contamination could be traced back in subsequent investigations to occasional beam excursions on the graphite support of the Mo sputter pellet. Using a Mo support the C content could be reduced to the 1–2 at.% level of the O contamination probably originating from residual gas components. Thus this simple ERDA technique could help to improve substantially the target quality as also shown in ref. [26] recently.

Another example concerns the production of a V target with high H content for determination of the electron momentum distribution of hydrogen in vanadium metal by  $(\gamma, e\gamma)$  spectroscopy [27]. For  $100 \text{ keV}$  synchrotron radiation the mean free path of recoil electrons is only of the order of  $10 \text{ nm}$ , therefore thin self-supported target foils of  $\text{VH}_x$  are needed. The foils were fabricated by electron beam evaporation and loaded afterwards with hydrogen by heating them in hydrogen atmosphere. H content in the foils was measured with ERDA again in transmission geometry using  $170 \text{ MeV } ^{127}\text{I}$  ions. It should be noticed that ERDA is more sensitive to H than to any other element. Energy spectra of these foils (Fig. 6) showed only 5 at.% H content, whereas about 50 at.% O could be detected. A possible explanation of the low hydrogen

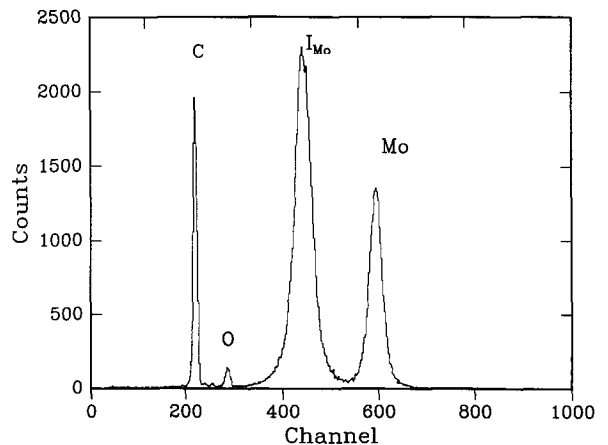


Fig. 5. Energy spectrum of transmission ERDA with  $140 \text{ MeV } ^{127}\text{I}$  beam on a  $^{100}\text{Mo}$  foil of about  $100 \mu\text{g}/\text{cm}^2$  thickness. Recoils and scattered projectiles ( $\text{I}_{\text{Mo}}$ ) are indicated. The C content measured is 75 at.% of Mo.

content could be the strong oxidation of the V foils, which seems to prevent a more effective hydrogen loading. Consequently the vacuum conditions of the production process have to be improved first. Thus with ERDA and heavy ion projectiles valuable information can be obtained on the light element content of thin foils even if only the energy of the recoils is measured.

### 5. ERDA with particle identification

Generally energy spectra of different recoil elements overlap due to finite sample thickness, therefore particle identification is necessary to separate the contributions of different elements. A typical example is the analysis of thin  $\text{TiN}_x\text{O}_y$ -Cu films, which are developed at the University of Munich as tandem solar absorbers with low emittance at high temperature [28].  $\text{TiN}_x\text{O}_y$  films of typically 100 nm thickness were deposited by activated reactive evaporation (ARE) on Cu coated glass substrates. To study the influence of oxygen and nitrogen content on the optical properties of these absorbers, samples with different partial pressures of both components during Ti evaporation were produced. The chemical composition of  $\text{TiN}_x\text{O}_y$  films has been measured with different methods, but the accuracy was partly limited due to peak overlap in AES [29] or the small sensitivity of RBS to N and O [30]. We used the ERDA method with 170 MeV  $^{127}\text{I}$  beam,  $37.5^\circ$  scattering angle and equal incidence and exit angle. Recoils were detected in the ionization chamber described above with an effective solid angle of 7.5 msr. In this geometry and with Cu being the heaviest component of the sample, according to Eq. (3), scat-

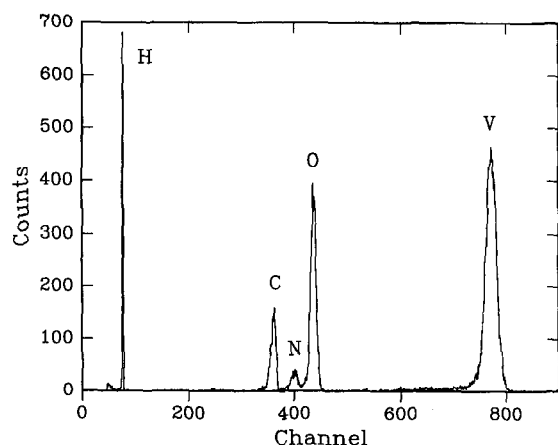


Fig. 6. Energy spectrum of transmission ERDA with 170 MeV I beam on  $\text{VH}_x$  foil. Recoils are indicated showing strong contamination. The hydrogen peak corresponds to  $x = 0.05$ .

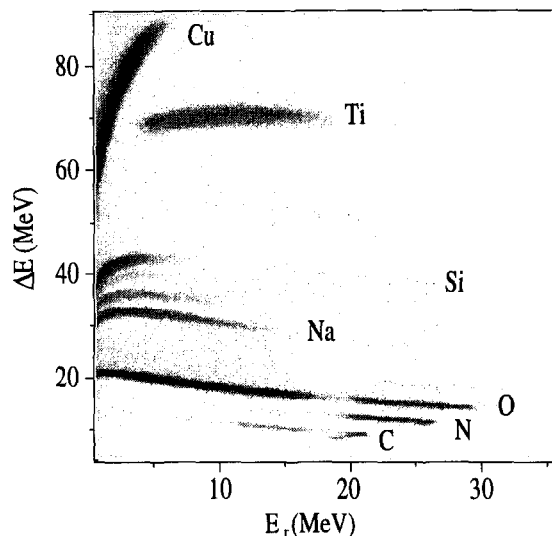


Fig. 7.  $(\Delta E, E_{\text{rest}})$  matrix of ERDA with 170 MeV I beam on a  $\text{TiN}_x\text{O}_y$  film. Components of the copper coated glass substrate are indicated.

tered projectiles could not reach the detector. To further avoid pileup of signals from recoiling ions the count rate of  $\Delta E$  pulses was kept below 500 Hz, corresponding to beam currents of less than 20 particle pA.

In the two-parameter plot of  $\Delta E$  and  $E_{\text{rest}}$  (Fig. 7) all three components of the  $\text{TiN}_x\text{O}_y$  film can be clearly identified as well as the copper coating and components of the glass substrate. Even a small C contamination, probably gettered from Ti during deposition, can be easily seen in the spectrum, although C is not fully stopped at the gas pressure of 70 mbar used in this measurement. Single elements can be resolved at least up to  $Z = 15$ , but recoils with different nuclear charges  $Z$  are only separated above a minimum energy of roughly 1 MeV/u. This condition can be performed with ERDA, in particular, if very heavy projectiles are used creating similar velocities for all recoil masses as mentioned above. The energy threshold for particle identification with this detector type, i.e. the minimum energy necessary to reach the  $E_{\text{rest}}$  part of the ionization chamber, requires also projectile energies above 1 MeV/u, which makes a large accelerator really necessary. In this study only the atomic ratio of the components was of interest, therefore no further data analysis was necessary and the information could be extracted on-line from the corresponding integrals in the  $(\Delta E, E_{\text{rest}})$  matrix. The accuracy was mainly limited by the statistical error and, for the O and N content, by surface contamination.

Another example where we used heavy ions for ERDA as well as for RBS was composition analysis of

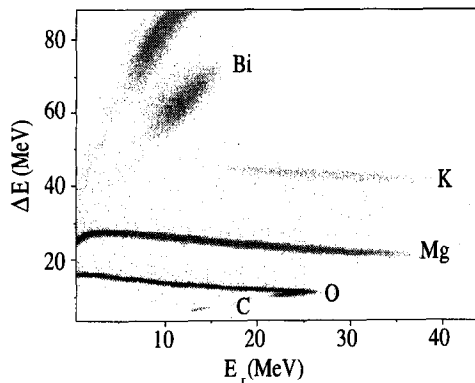


Fig. 8. ( $\Delta E$ ,  $E_{\text{rest}}$ ) matrix of ERDA with 170 MeV I beam on a BaBiKO film. MgO substrate and C contamination are indicated.

BaBiKO, one of the highest-temperature oxide superconductors ( $T_c \approx 30$  K) apart from the layered cuprates. Here in Munich at the Technical University epitaxially grown BaBiKO films on MgO substrates are fabricated by a thermal co-evaporation process [31]. In the beginning these films did not show superconductivity. It was suspected either the stoichiometric composition was wrong or some contamination occurred during the production process. First to control the Ba to Bi ratio, the high mass resolution of RBS with  $^{16}\text{O}$  of 25 MeV was used. Then ERDA was made with 170 MeV  $^{127}\text{I}$  ions using our ionization detector, where besides K and all lighter elements also Bi could be seen separated in the ( $\Delta E$ ,  $E_{\text{rest}}$ ) matrix (Fig. 8). Note that Bi recoils are well below the energy threshold for particle identification in our ionization detector. From integrals in the two-parameter spectra and peak integrals of the RBS spectra the composition of the films could be deduced showing the correct stoichiometry. But in the two-parameter plot also a very strong C contamination could be detected, in some films even a ratio of K:C = 1:1 was measured. This contamination could be traced back to the oil diffusion pump used in the production chamber. After replacement by a completely oil-free pumping system superconducting films could be produced with critical temperatures up to 23 K.

## 6. ERDA with position resolution

Whereas in the examples above depth resolution played only a minor role, it is of great importance in applications, where the contents of a certain element in different sample layers have to be measured. High sensitivity, i.e. large detector solid angle, can be combined with high depth resolution only if the related kinematic energy shift is compensated as was discussed

in section 2. The horizontal acceptance angle of our ionization detector is about  $6^\circ$  for example which causes an energy spread  $\delta E$  of 18% precluding good depth resolution. Thus we use the position sensitivity of our ionization detector to measure the recoil scattering angle together with energy and Z-information for every detected particle. In further data processing which is described in detail elsewhere [23] the energy of each event is shifted corresponding to one common scattering angle.

An application of the resulting depth resolution is the analysis of the oxygen concentration in metallic films on oxide substrates which have been prepared at the Hahn-Meitner-Institut in Berlin [32]. ERDA was performed with 170 MeV  $^{127}\text{I}$  ions and recoils were detected at  $37.5^\circ$  mean scattering angle. Due to the large solid angle of the ionization detector (7.5 msr) total fluences of  $10^{12}$  at./ $\text{cm}^2$  were sufficient for these measurements. The energy spectrum of recoil oxygen ions from an epitaxial Nb film on  $\text{Al}_2\text{O}_3$  substrate is shown in Fig. 9 which has been corrected for kinematic energy shifts. The Nb film was covered with a thin Au layer immediately after evaporation deposition in order to prevent the oxidation on air. Also shown in the figure is a simulation of the data with the program RUMP [33] used in a slightly modified version for spectrum analysis so far. The normalization was derived from an adjustment of the fit to the  $\text{Al}_2\text{O}_3$  substrate. In the expanded part of Fig. 9 an additional oxygen peak can be seen from surface contamination, the estimated depth resolution at the surface is around 20 nm. In the simulation indicated by the smooth line an oxygen-free Au layer of 20 nm thickness has been assumed, whereas the Nb film was best fitted with a constant oxygen concentration of about 1.5 at.%. This was a surprising result. Because of the UHV conditions during film preparation an oxygen-free Nb film had been expected. Besides the possibility that the oxygen contamination occurred during film production, there is, in the present case, also a chance of contamination in a later stage since the film had been charged with hydrogen. This example clearly demonstrates the possibilities of ERDA with good depth resolution for oxygen profiling of thin films which quite often is a problem on substrates with high oxygen content. Here one takes advantage of this high content to normalize the data on a known oxygen concentration.

Depth resolution is also a prerequisite for a very different application of the ERDA technique, where radiation induced changes (sputtering or mixing) of thin surface layers will be measured. In this case heavy ions are used to simultaneously sputter and analyse the surface. Recently, Sudgen et al. [34] studied with this method sputter effects by 30 MeV Cl ions on thermally grown  $\text{SiO}_2$  films at UHV conditions. Using also this method we have started measurements of sputter yields

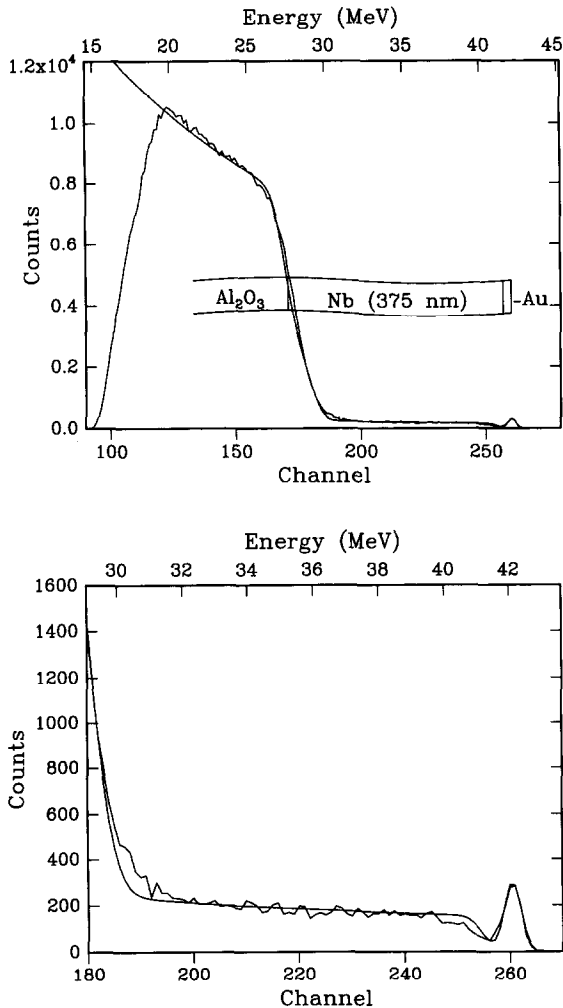


Fig. 9. (Upper part) O recoil energy distribution from a Nb film on  $\text{Al}_2\text{O}_3$  covered with Au. ERDA was measured with 170 MeV I beam. Energies are corrected for kinematic shift. (Lower part) expanded view of the high energy part showing O peak from surface contamination.

with high energetic very heavy ions for two reasons. First we are interested in the tolerable ion fluence to prevent sample alterations during heavy ion ERDA, secondly it is of basic interest, if enhanced sputter yields known for insulating materials due to electronic effects [19] can be also measured for metallic materials. In order to answer the first question a multilayer target consisting of 15 nm Al, 30 nm  $^{63}\text{Cu}$ , 30 nm Al and 30 nm  $^{63}\text{Cu}$  layers on Si substrate has been irradiated with 200 MeV Au ions and currents of 0.5 particle nA [23]. The 30 nm Al layer was thought to be not affected by sputtering acting as a reference for normalization. Besides the Al and Cu peaks additionally in each interface O, N and C contamination peaks were seen with concentrations down to  $2 \times 10^{14}$  at./ $\text{cm}^2$ . The depth

resolution achieved at  $3.5^\circ$  incidence angle was about 7 nm for the Al surface layer and about 5 nm for the Cu layer near the surface, thus recoils of the two Al layers could be easily separated and their areal densities compared for increasing ion fluence. No change of the peak area ratio could be observed up to a maximum fluence of  $4 \times 10^{14}$  at./ $\text{cm}^2$  which is more than ten times the fluence usually needed for sample analysis. Therefore this heavy ion irradiation performed at our standard vacuum conditions, i.e.  $5 \times 10^{-7}$  mbar, did not create a measurable sputter effect. This might be different for nonmetallic samples. A new UHV setup is in preparation to continue these investigations at well defined surface conditions.

Surface depth resolution of our ERDA system with correction of the kinematic energy spread is limited by the detector energy resolution (including entrance foil effects) which has been seen in routine operation to be 0.8% for O or Al. Best values of energy resolution measured with an ionization detector are 0.4% [35], thus substantial improvements of depth resolution can be expected only of different energy detection methods. Dollinger et al. [36] have demonstrated nearly atomic resolution, namely 3.5 Å, using the Munich Q3D magnetic spectrograph with its superb energy resolution of 0.05%. This resolution could be obtained for a solid angle of about 2 msr due to special multipole elements in this spectrograph to correct for kinematic energy shifts. It points out also the excellent beam quality which can be delivered by an electrostatic accelerator.

## 7. Blocking ERDA

The two-dimensional position resolution of our detection system offers the opportunity to try a new variety of ERDA making use of the blocking effect which we call blocking ERDA therefore. Recoil atoms starting in single-crystalline materials in direction of crystal axes or planes are blocked and give rise to very distinct angular distributions. Since blocking trajectories can be formally treated as the time reversals of channeling trajectories angular distributions of blocking are identical to the channeling angular distributions for the same scattering conditions [37]. Impressive blocking patterns have been seen with radiation-sensitive films, but for quantitative structural analysis suited detection systems were lacking. Nuclear physicists, however, used this effect since its discovery to measure nuclear lifetimes in the range of  $10^{-17}$  to  $10^{-19}$  s [38]. Recently a Bragg ionization chamber in combination with a position sensitive detector has been applied for this purpose [39].

In order to test, if the position resolution of our ionization detector is sufficient to resolve blocking

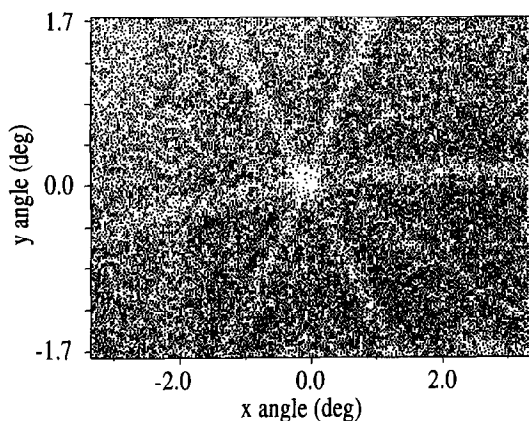


Fig. 10. Blocking pattern of Si(111) single crystal irradiated by 170 MeV I ions. Si recoils shown for a 0–100 nm depth window are blocked by a  $\langle 111 \rangle$  axis and related planes.

patterns, the (111) surface of a 3 mm thick Si single crystal was irradiated by 170 MeV I ions. The crystal surface was oriented to have a  $\langle 111 \rangle$  axis pointing at the center of the detector entrance window. In Fig. 10 a two-parameter plot of the  $x$  and  $y$  position of Si recoils calibrated in corresponding angles is shown with a depth window set on the first 100 nm. Clearly the blocking effect of the  $\langle 111 \rangle$  axis and corresponding planes can be seen. The slight  $y$  distortion is an artificial effect caused by the measuring method which can be corrected using the  $(x, y)$  calibration. From this matrix axial and planar values of  $\chi_{\min}$  and  $\psi_{1/2}$  could be extracted as described in ref. [40]. This new ERDA technique which allows to measure blocking patterns of different sample components simultaneously has to be further tested for its capabilities in structural analysis. Beam induced damage in particular has been found to limit the usefulness of channeling ERDA for this application, if a TOF system with small solid angle is used [18]. Blocking ERDA with a large solid angle detector could overcome this limitation. Moreover it opens the possibility to study systematically the damaging power of heavy ions in single crystals looking into dechanneling effects during irradiation. Pioneering work in this field has been done by Karamyan [41] recording the blocking patterns with track detectors.

## 8. Summary

We have tried to give some typical examples of problems in thin film analysis which can be very well solved with heavy ion ERDA. Cross section dependence and scattering angle restriction favor very heavy ions as projectiles for ERDA, whereas detection of recoiling sample atoms enables particle identification.

For this purpose a large tandem accelerator and an ionization detector seem to form a perfect team. High energetic projectiles are necessary for good energy and particle resolution of ionization detectors which in turn have two very desired properties for ERDA: large solid angle and position resolution. This results in combination with the very good beam quality of a tandem accelerator in high depth resolution and sensitivity, values below 10 nm and  $10^{14}$  at./cm<sup>2</sup> could be achieved, respectively. Although energy detection of recoils only has been shown to give valuable information in target foil analysis, for most applications a more complete characterization of recoils has to be done. Particle resolution allows to unfold the energy spectra of different elements at least up to  $Z = 15$ , whereas additional position resolution besides improving depth resolution opens the possibility of recording blocking patterns. As a result the ERDA method cannot only be applied for depth profiling and structural analysis of materials but also in basic research of sputtering or damaging with heavy ions.

## Acknowledgement

We would like to acknowledge the fruitful cooperation with all the people who have prepared our thin film samples: F. Baudenbacher, S. Blässer, Th. Grassl, Th. Eisenhammer, M. Lazarov and H.J. Maier. We wish also to acknowledge the helpful discussions with F. Bell and the permanent support by W. Hering.

## References

- [1] W.K. Chu, J.W. Mayer and M.A. Nicolet, Backscattering Spectrometry (Academic Press, New York, 1978).
- [2] L.C. Feldman, J.W. Mayer and S.T. Picraux, Materials Analysis by Ion Channeling (Academic Press, New York, 1982).
- [3] L.C. Feldman and J.W. Mayer, Fundamentals of Surface and Thin Film Analysis (North-Holland, New York, 1986).
- [4] B.L. Doyle and P.S. Peercy, Appl. Phys. Lett. 34 (1979) 811.
- [5] J. L'Ecuyer, C. Brassard, C. Cardinal and B. Terreault, Nucl. Instr. and Meth. 149 (1978) 271.
- [6] C. Nölscher, W. Schmidt, K. Brenner, V. Brückner, M. Lehmann, P. Müller and G. Saemann-Ischenko, in: Nuclear Physics Methods in Materials Research, eds. K. Bethge, H. Baumann, H. Jex and F. Rauch (Vieweg, Braunschweig, 1980) p. 349.
- [7] R. Groleau, S.C. Gujrathi and J.P. Martin, Nucl. Instr. and Meth. 218 (1983) 11.
- [8] J.P. Thomas, M. Fallavier, D. Ramdane, N. Chevarier and A. Chevarier, *ibid.*, p. 125.
- [9] B.L. Doyle, P.S. Peercy, T.J. Gray, C.L. Cocke and E. Justiniano, IEEE Trans. Nucl. Sci. NS-30 (1983) 1252.
- [10] G. Dollinger, T. Faestermann and P. Maier-Komor, Nucl. Instr. and Meth. B 64 (1992) 422.

- [11] M. Petrascu et al., Nucl. Instr. and Meth. B 4 (1984) 396.
- [12] A.M. Behrooz, R.L. Headrick, L.E. Seiberling and R.W. Zurmühle, Nucl. Instr. and Meth. B 28 (1987) 108.
- [13] E. Henschel, R. Kotte, H.G. Ortlepp, F. Stary and D. Wohlfarth, Nucl. Instr. and Meth. B 43 (1989) 82.
- [14] B. Gebauer, D. Fink, P. Goppelt, M. Wilpert and Th. Wilpert, Nucl. Instr. and Meth. B 50 (1990) 159.
- [15] W.M.A. Bik, C.T.A.M. de Laat and F.H.P.M. Habraken, Nucl. Instr. and Meth. B 64 (1992) 832.
- [16] J.P. Stoquert, G. Guillaume, M. Hage-Ali, J.J. Grob, C. Ganter and P. Siffert, Nucl. Instr. and Meth. B 44 (1989) 184.
- [17] R. Yu and T. Gustafsson, Surf. Sci. 177 (1986) L987.
- [18] C. Janicki, P.F. Hinrichsen, S.C. Gujrathi, J. Brebner and J.-P. Martin, Nucl. Instr. and Meth. B 34 (1988) 483.
- [19] L.E. Seiberling, C.K. Meins, B.H. Cooper, J.E. Griffith, M.H. Mendenhall and T.A. Tombrello, Nucl. Instr. and Meth. 198 (1982) 17.
- [20] U. Hardy, D. Groult, M. Hervieu, J. Provost, B. Raveau and S. Bouffard, Nucl. Instr. and Meth. B 45 (1991) 472.
- [21] U. Quade, K. Rudolph and G. Siegert, Nucl. Instr. and Meth. 164 (1979) 435.
- [22] W. Assmann, Nucl. Instr. and Meth. B 64 (1992) 267.
- [23] W. Assmann, P. Hartung, H. Huber, P. Staat, Ch. Steinhäusen and H. Steffens, Nucl. Instr. and Meth. B 85 (1994) 726.
- [24] S.C. Gujrathi, D.W. Hetherington, P.F. Hinrichsen and M. Bentourkia, Nucl. Instr. and Meth. B 45 (1990) 260.
- [25] H.J. Maier, Nucl. Instr. and Meth. A 303 (1991) 172.
- [26] Jai Pal, D. Kabiraj and D.K. Avasthi, Nucl. Instr. and Meth. A 334 (1993) 196.
- [27] F.F. Kurp, Th. Tschentscher, W. Assmann, F. Bell and J.R. Schneider, Proc. 13th Gen. Conf. Cond. Matter Div. EPS, Regensburg, Germany, 1993, p. 1273.
- [28] M. Lazarov, B. Röhle, T. Eisenhammer and R. Sizmann, Proc. SPIE 1536 (1991) 183.
- [29] B.J. Burrow, A.E. Morgan and R.C. Ellwanger, J. Vac. Sci. Technol. A 4(6) (1986) 2463.
- [30] F.L. Freire Jr., B.K. Patnaik, C.V. Barros Leite, I.J.R. Baumvol and W.H. Schreiner, Nucl. Instr. and Meth. B 40/41 (1989) 769.
- [31] Th. Grassl, Diploma Thesis, TUM München (1993).
- [32] S. Blässer, Ph.D. Thesis, Universität Konstanz (1993).
- [33] L.R. Doolittle, Nucl. Instr. and Meth. B 9 (1985) 344.
- [34] S. Sugden, C.J. Sofield and M.P. Murrell, Nucl. Instr. and Meth. B 67 (1992) 569.
- [35] A. Oed, P. Geltenbort, F. Gönnerwein, T. Manning and D. Souque, Nucl. Instr. and Meth. 205 (1983) 455.
- [36] G. Dollinger, Th. Faestermann, C.M. Frey, A. Bergmaier, Th. Fischer, R. Schwarz and E. Schwabedissen, Nucl. Instr. and Meth. B 85 (1994) 786.
- [37] J. Lindhard, K. Dan. Vidensk. Selsk. Mat. Fys. Medd. 34 (1965) 14,1.
- [38] W.M. Gibson, Ann. Rev. Nucl. Sci. 25 (1975) 465.
- [39] E. Fuschini et al., Phys. Rev. C 46 (1992) R25.
- [40] F. Malaguti et al., Europhys. Lett. 12 (1990) 313.
- [41] S.A. Karamyan, Nucl. Instr. and Meth. B 51 (1990) 354.